Lycium barbarum Polysaccharide Improves Bipolar Pulse Current-Induced Microglia Cell Injury Through Modulating Autophagy

Man Bie,* Yi Lv,† Chaoran Ren,* Feiyue Xing,† Qi Cui,* Jia Xiao,†‡ and Kwok Fai So*‡§¶

*GMH Institute of CNS Regeneration, Guangdong Medical Key Laboratory of Brain Function and Diseases,
Jinan University, Guangzhou, China
†Department of Immunobiology, Institute of Tissue Transplantation and Immunology, Jinan University, Guangzhou, China
‡Department of Anatomy, The University of Hong Kong, Hong Kong SAR, China
§Department of Ophthalmology, The University of Hong Kong, Hong Kong SAR, China
¶State Key Laboratory of Brain and Cognitive Sciences, The University of Hong Kong, Hong Kong SAR, China

Blindness and visual impairments are heavy loads for modern society. Visual prosthesis is a promising therapy to treat these diseases. However, electric stimulation (ES)-induced damage of the optic nerve and adjacent cells are problems that must not be overlooked. In the current study, we aimed to investigate the effects of ES on cultured microglia cells and the potential protective mechanisms from a natural compound *Lycium barbarum* polysaccharide (LBP). Cellular injuries were induced by 9 mA bipolar pulse current in BV-2 cells for 15 min. Treatment with LBP alone or in association with either autophagic inhibitor 3-MA or autophagic agonist rapamycin was preadded for 2 h before the ES challenge. After that, morphological and molecular changes of the cells were measured at 2 h or 6 h postchallenges. We found that ES induced evident morphological and pathological changes of BV-2 cells, including oxidative stress, inflammation, and apoptosis. Pretreatment with LBP significantly attenuated these injuries with enhanced endogenous autophagy. When cellular autophagy was inhibited or enhanced by corresponding drug, the protective properties of LBP were partly inhibited or maintained, respectively. In addition, we demonstrated that ERK and p38 MAPK exerted diversified roles in the protection of LBP against ES-induced cellular damages. In conclusion, LBP improves bipolar pulse current-induced microglia cell injury through modulating autophagy and MAPK pathway.

Key words: *Lycium barbarum* polysaccharide (LBP); Microglia injury; Electric stimulation (ES); Autophagy

INTRODUCTION

Blindness is a severe public health problem with a heavy social burden in health and economics. According to the World Health Organization, the number of people of all ages visually impaired is estimated to be 285 million globally, of whom 39 million are blind (26). Up to 2010, the main causes of blindness have included cataract (51%), glaucoma (8%), age-related macular degeneration (5%), childhood blindness and corneal opacities (4%), uncorrected refractive errors and trachoma (3%), diabetic retinopathy (1%), and undetermined causes (21%) (25). With the appearance of the first neural prosthesis in the 1970s, this field has grown to a $4.7 billion industry with an annual growth rate of 20% (3). Among the most exciting developments is visual prosthesis, which was designed to provide artificial visuality for the blind, resulting in increased independent living and quality of life (21). Although microelectronics have been used to treat blindness, several problems during the application, particularly its safety issue and underlying mechanisms, remain to be fully addressed.

For an effective and safe treatment, microelectronic devices should be implanted in the body for decades with adequate power supply and no potential corrosion and infection (24). However, it has been reported that activated electrodes may induce a redox reaction and electrolytic corrosive effects. Importantly, when microelectronic arrays were implanted on the optic nerve 1.0 mm behind the eyeball, the effects of the electric current on the adjacent neurons and glia cells are still uncertain. Moreover, it has been found that there was a glia cell layer between the implanted device and the retinal neurons, acting as an insulating layer in the retinal implant (16). This cell layer may decrease the efficacy of electrical signals, and therefore a

larger current is needed to achieve the expected therapeutic outcomes, which probably leads to a serious oxidation reaction and electrocorrosion. In the retina, microglia is the resident immune effector cell, which has been implicated as a contributor to these neurotoxic products once completely activated (1,15). Thus, elucidating the effects of the electric current on microglial fates is vital for the future development and application of visual prostheses.

Autophagy is an intracellular catabolic pathway, which degrades cell components, toxic aggregates, and damaged organelles to recycle them as basic building blocks for the maintenance of cellular homeostasis (33). During autophagy, intact organelles (such as mitochondria) and portions of the cytosol are sequestered into a double-membrane vesicle to form an autophagosome, which matures later and fuses with an endosome and/or lysosome to form an autolysosome (18). Then the cargo is broken down, and the macromolecules are transported back into the cytosol for reuse (18). Autophagy represents a cytoprotective response in many cell types, and its deregulation is implicated in many diseases, such as infectious diseases, cancer, and neurodegeneration (2,11). In the neuronal system, it protects the retinal ganglion cells (RGCs) from optic nerve axotomy (19), and its overexpression or insufficiency may induce neuronal death and neurological disorders (7,13).

Lycium barbarum (Wolfberry) is a traditional Chinese medicine used for centuries in the Eastern world to maintain eye health and nourish the liver and kidneys and to balance "Yin" and "Yang" in the body (4). Our previous studies found that the polysaccharide part of Wolfberry (LBP) could reduce neuronal damage, blood–retinal barrier disruption, and oxidative stress in retinal ischemia/reperfusion injury (14) and antagonize glutamate excitotoxicity in rat cortical neurons (8). However, whether it is effective in reducing electric damage (e.g., oxidative stress and apoptosis) of the microglial cell is unknown. In the current study, we aimed to examine the cellular and molecular events after bipolar pulse current (or electric stimulation, ES) treatment in microglial cells in vitro. The role of autophagy during the damaging and recovery processes will be studied in detail.

MATERIALS AND METHODS

Chemicals and Reagents

The preparation for LBP extracts (from *Lycium barbarum*, Ning Xia Huizu Autonomous Region, People's Republic of China) was the same as reported previously (8). All cell culture consumables and reagents were bought from either Corning (Corning, NY, USA) or Gibco (Carlsbad, CA, USA). Antibodies against catalase (CAT) and ED1 (cluster of differentiation 68; CD68) were bought from Abcam (Cambridge, UK). Beclin-1, autophagy protein 5 (Atg5), nucleoporin p62 (p62), light chain 3B (LC3B), inducible nitric oxide synthase (iNOS), total p38 mitogen-activated protein kinase (MAPK),

phosphorylated p38 MAPK at Thr180/Tyr182, total extracellular signal-regulated kinase (ERK), and phosphorylated ERK at Tyr204 antibodies were bought from Cell Signaling (Danvers, MA, USA). Autophagic inhibitor 3-methyladenine (3-MA) and agonist rapamycin were purchased from Sigma-Aldrich (St. Louis, MO, USA).

Cell Culture and ES

Mouse normal brain microglia BV-2 cell line was supplied by the Cell Bank of Type Culture Collection of Chinese Academy of Sciences (Shanghai, China). BV-2 cells were cultured in Dulbecco's modified Eagle's medium (DMEM) with 10% (v/v) fetal bovine serum (FBS) at 37°C with 5% CO_2 supply using a cell incubator (Thermo Fisher, Waltham, MA, USA). Before every treatment, the cells reached a confluence of 60–70%. For the pretreatment with 50 µg/ml LBP, 1× phosphate buffered saline (PBS) dissolved LBP was added 2 h before the ES challenge. For 3-MA or rapamycin treatment, 10 mM 3-MA (in PBS) or 100 nM rapamycin [in dimethyl sulfoxide (DMSO)] was added to the culture medium 2 h before the ES (with or without LBP cotreatment).

ES of BV-2 cells was performed as previously reported with minor modifications (6). Briefly, ES was applied across a 3.5-mm dish in which two platinum-iridium alloy electrodes set on opposite sides of the dish are in contact with the medium. The ends of the electrodes were connected with the electric stimulator. The bipolar pulse current needed a stimulus isolator to magnify and was checked by oscilloscope in a real-time manner. Each stimulation pulse (15 min, 9 mA) was sufficient to induce potential damage in BV-2 cells, according to our pilot study (data not shown). The entire ES was performed in a biosafety cabinet where the sham groups also received sham treatment for 15 min, then all cells were incubated a 37°C, 5% CO_2 incubator for 2 or 6 h. The following stimulation paradigms were used. Each episode consisted of 300 biphasic pulses at 1 Hz (0.5 ms phase duration of each single phase and 0.5 ms interval-phase delay). The ES challenge was generated by a Master-8 pulse stimulator (AMPI, Jerusalem, Israel), a stimulus isolator A365 (World Precision Instruments, Sarasota, FL, USA), and a TDS 1001B oscilloscope (Tektronix, Beaverton, OR, USA). Two and 6 h after the stimulation, cells were subjected to various cellular and molecular studies. Pattern of ES and experiment design are shown in Figure 1.

Quantification of Apoptotic Cells

Two and 6 h after the stimulation, Hoechst 33342 (5 µg/ml) and propidium iodide (5 µg/ml) were added to each dish to stain live and dead cells. The cell population was separated into three groups: live cells showed only a low level of fluorescence; apoptotic cells showed a higher level of blue fluorescence, and dead cells showed
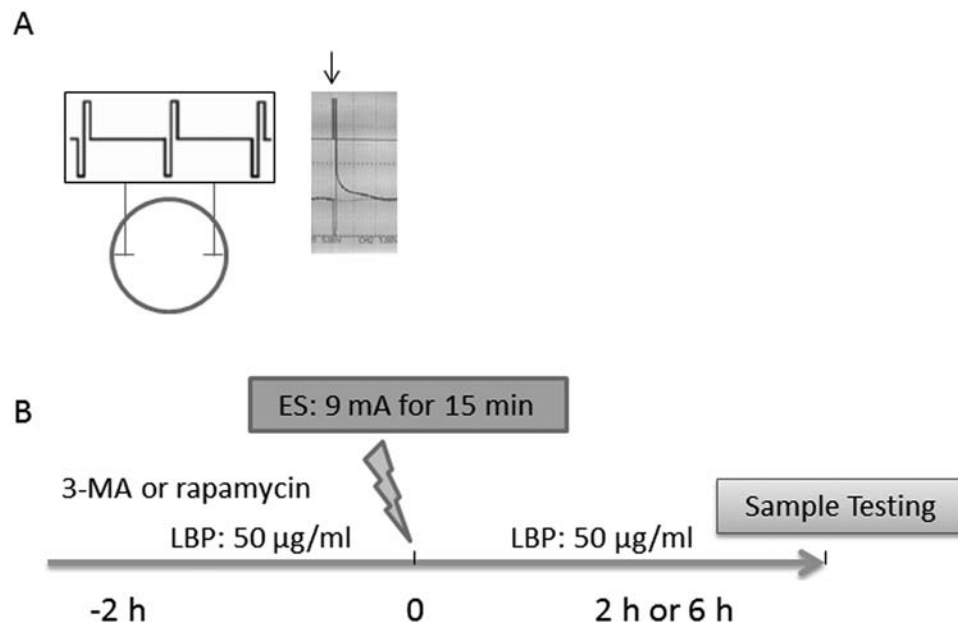
Figure 1. Pattern of ES on microglia BV-2 cells. (A) Two platinum-iridium alloy electrodes set at opposite sides of the dish are in contact with the medium. ES was given at 9 mA for 15 min, by first negative and then later positive bipolar square pulses. The arrow is representative of the pulse. (B) Flow chart of ES. LBP work concentration is 50 μg/ml, pretreated before ES for 2 h. Two or 6 h later, cells were collected for the following measurements. 3-MA, 3-methyladenine.

low-blue and high-red fluorescence. Stained cells were observed and quantified by two independent cell biologists without knowing the grouping. The results were expressed as the percentage of apoptosis (PA): PA = apoptotic cell number/total cell number × 100% (30).

Caspase 3/7 Activity Measurements

Activities of caspases 3/7 from cell lysates (collected by RIPA buffer; Sigma-Aldrich) were measured using Caspase-Glo 3/7 Assay Systems (Promega, Madison, WI, USA) according to the user's manual. The luminescence was read in a Glomax luminometer (Promega) and expressed as fold change in caspase 3/7 activity from the control.

Live Cell Imaging and LC3 Fluorescence

Time lapse live cell image after ES was performed on an Axio Observer Z1 live cell station (Carl Zeiss, Oberkochen, Germany). The dynamic changes of expression and localization of live cell LC3 protein was visualized by transfecting mouse LC3-green fluorescent protein (GFP) plasmid (a kind gift from Dr. Rongrong He, Pharmacy College, Jinan University, China) using lipofectamine 3000 (Life Technologies, Shanghai, China) for 24 h.

Western Blot

Western blot analyses of cell lysates were performed as described previously (28). Glyceraldehyde-3-phosphate dehydrogenase (GAPDH; Cell Signaling) was used as the internal control for all experiments.

Statistical Analysis

Data from each group were expressed as means ± SEM ($n = 4$ for each group). The statistical significance of differences between groups was tested using one-way analysis of variance (ANOVA with Bonferroni correction of the Student's t-test as a post hoc test) or Student's t-test if only two groups were being compared. A value of $p < 0.05$ was considered to be statistically significant (Prism 5.0; Graphpad Software, Inc., San Diego, CA, USA).

RESULTS

Pretreatment With LBP Ameliorated ES-Induced BV-2 Cellular Necrosis and Apoptosis After ES

Two hours after the ES challenge (9 mA for 15 min), the BV-2 cells shrank, which was aggravated at 6 h after the challenge (Fig. 2A, B). Accordingly, the number of necrotic and apoptotic cells was significantly increased ($p < 0.001$) (Fig. 2). When the cells were pretreated with LBP, both the morphology and necrotic/apoptotic status of the cells after ES was significantly ameliorated to control-comparable levels without affecting the healthy cells ($p < 0.05$) (Fig. 2).
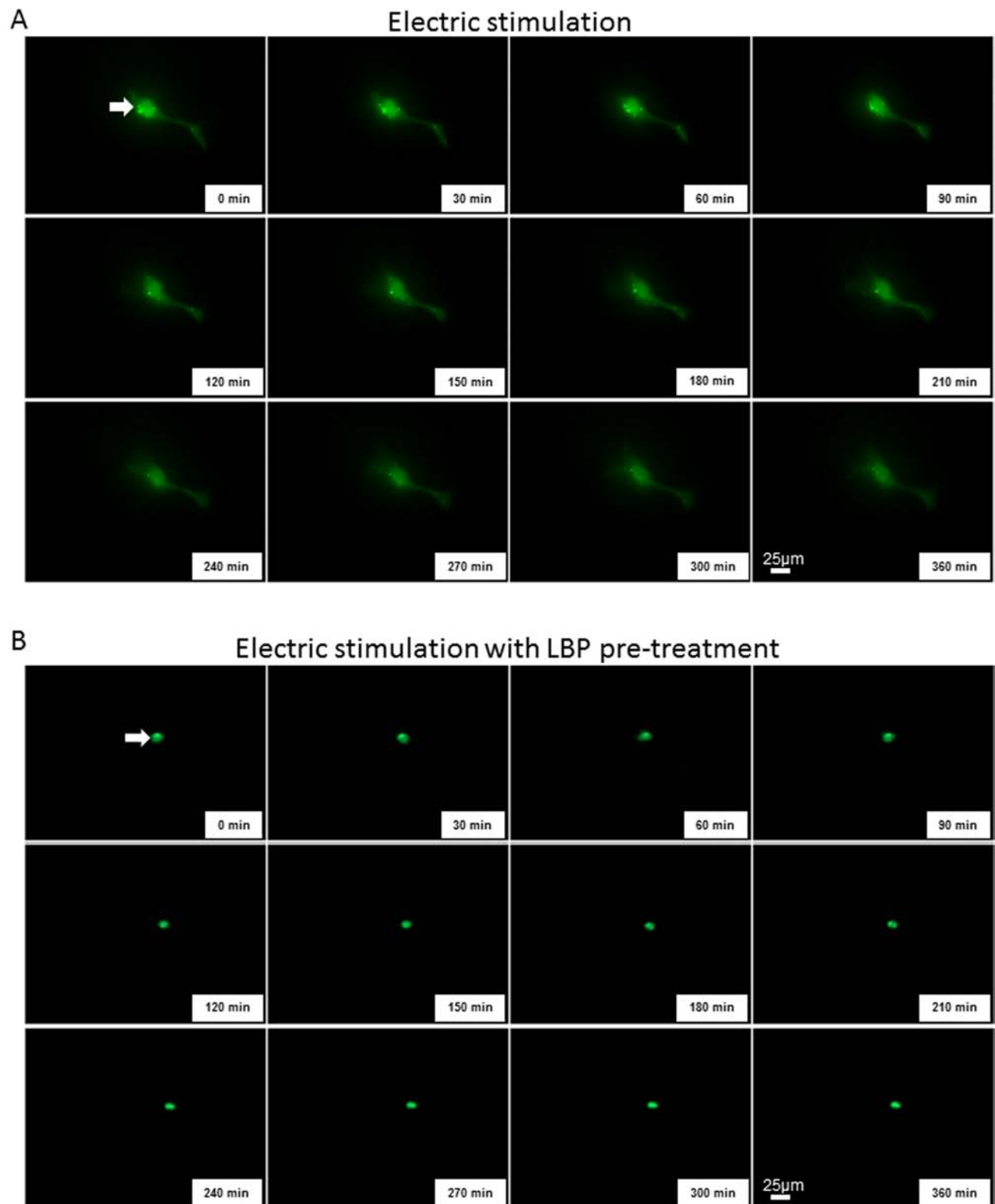
Pretreatment With LBP Stabilizes the Expression and Cellular Localization of LC3B After ES

To examine the effects of ES and LBP pretreatment on cellular autophagy, the dynamic cellular localization and expression level of key autophagic protein LC3B was visualized by a time-lapse fluorescence microscopy
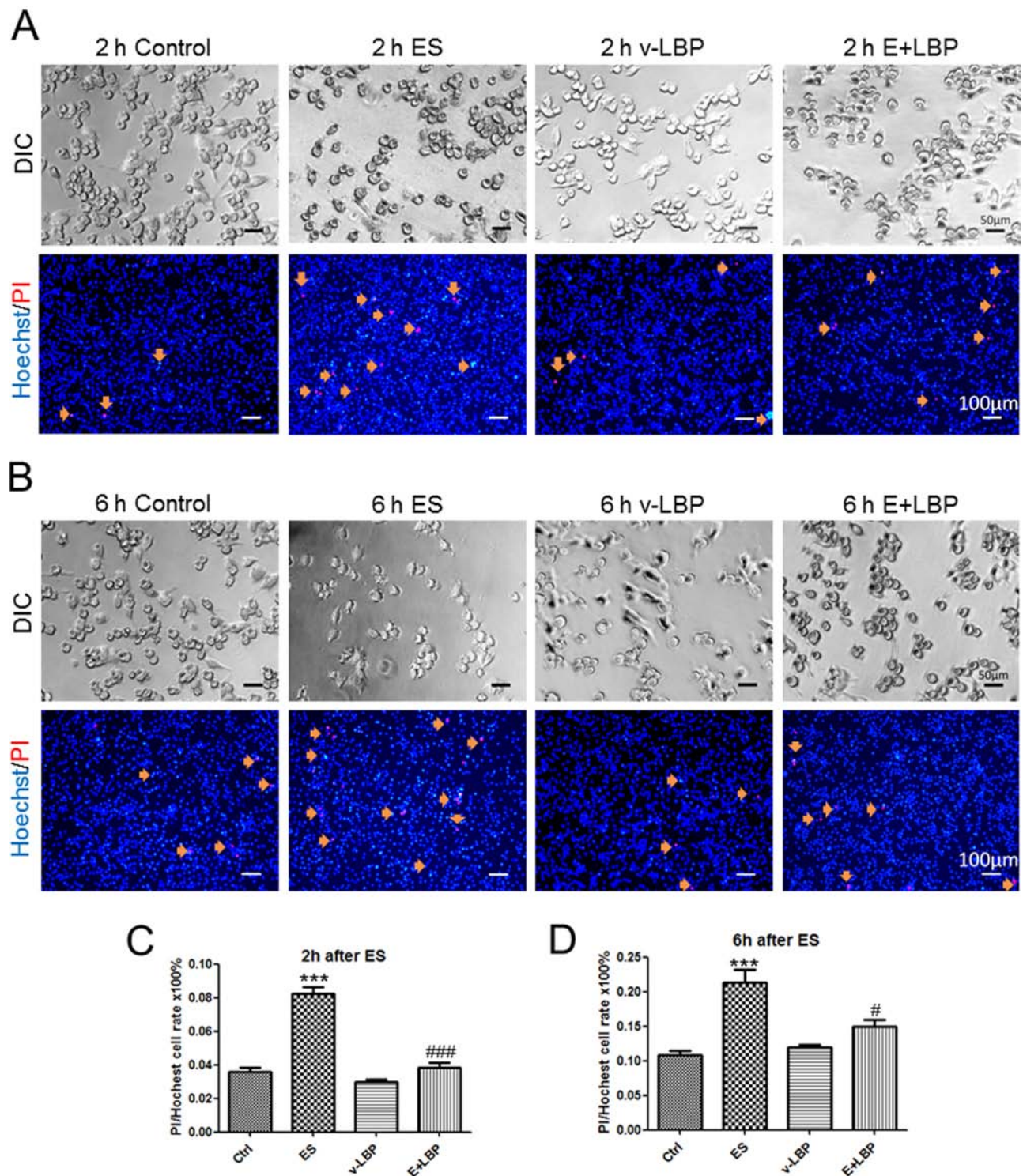
Figure 2. Ameliorative effects of LBP on the electric stimulation-induced apoptosis and necrosis of BV-2 cells. (A) Differential inter-ference contrast (DIC) photos (200× magnification) show the representative morphology of normal BV2 microglia of control group, ES 9 mA-15 min-2 h group, vehicle-LBP group, and ES + LBP group after ES 2 h or 6 h. LBP was pretreated before ES 2 h at 50 μg/ml. (B) Fluorescent photos (100× magnification) show the propidium iodide (PI) and Hoechst double-labeled cells of the four groups. Orange arrows indicate the apoptosis or necrosis cells (scale bar: DIC 50 μm, fluorescence 100 μm). (C) and (D) Quantified percent-ages of (A) and (B), respectively ($n = 4$ for each group). After ES, the number of apoptosis and necrosis cells increased while LBP significantly decreased the damage. ***Significant change ($p < 0.001$) between control and ES groups. # and ###Significant changes ($p < 0.05$ and $p < 0.001$) between ES group and ES + LBP groups.

Figure 3. LBP stabilizes the expression and cellular localization of LC3B in BV-2 microglia cells. Representative 6-h time-lapse fluorescence pictures showing the expression and localization of light chain 3B (LC3B) after transfecting with mouse LC3B-GFP plasmid for 24 h before the electric stimulation (A) without LBP pretreatment or (B) with LBP pretreatment. Arrows indicate the localization of LC3B fluorescent signals. Magnification: 400×.
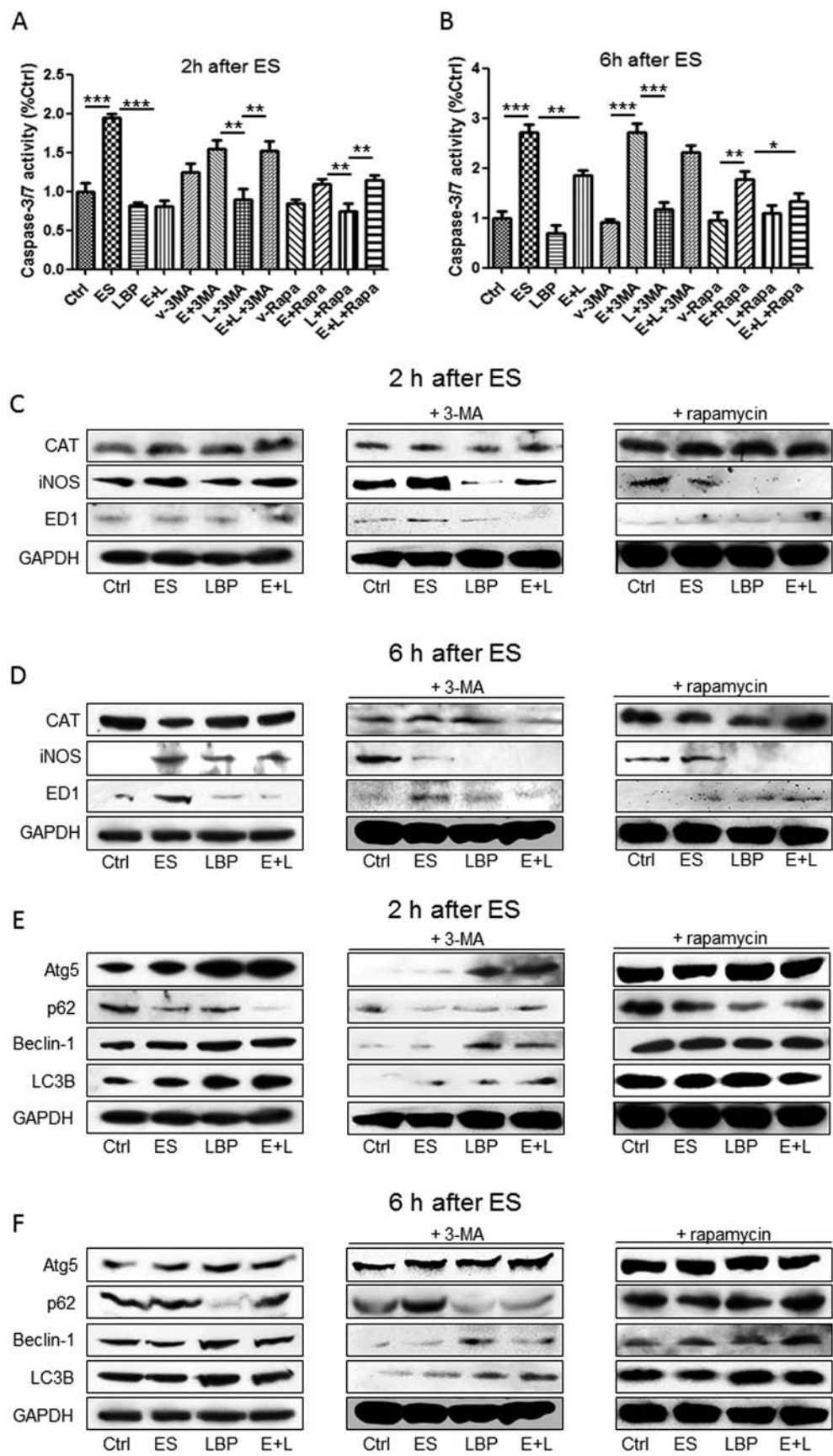
using LC3B-GFP plasmid. It was shown that before ES, when there was no LBP pretreatment, the level of LC3B in BV-2 cell was low and the cellular localization was spread. Two-hour pretreatment with LBP concentrated the LC3B expression and localization (Fig. 3). As time went on, the level of LC3B was slightly increased in the ES-only group but showed no obvious change in the ES+LBP group at 2 h postchallenge. At 6 h post-ES challenge, the level of LC3B was evidently inhibited, while the pretreatment with LBP still maintained the LC3B level and localization at a 0-min comparable level (Fig. 3 and supplementary videos 1 and 2 at https://drive.google.com/file/d/0B75g-qH9l7QlbkFvcUd-BOVlJZTQ/view?usp=sharing and https://drive.google.com/file/d/0B75g-qH9l7QlTGFCQWJRMENVRDA/view?usp=sharing).

Antiapoptotic and Antioxidant Effects of LBP
on ES-Induced BV-2 Cell Damage
Were Mediated by Autophagy

To correlate the autophagic regulating function and ameliorative effects of LBP on ES-induced cellular damages, we applied the autophagic inhibitor 3-MA and agonist rapamycin in the study. Results of caspase 3/7 activity showed that ES significantly increased the activity of caspase 3/7 in BV-2 cells, both at 2 h and 6 h postchallenge (Fig. 4A). Pretreatment with LBP significantly reduced the caspase 3/7 activity, when compared with the ES group. When 3-MA was applied, it partly abolished the beneficial effects of LBP pretreatment on the reduction of caspase 3/7 activity (Fig. 4A). When endogenous autophagy was enhanced by rapamycin, an inhibitor of the autophagic suppressor mammalian target of rapamycin (mTOR), the apoptotic-ameliorative effects of LBP was partly impaired at 2 h postchallenge but was further enhanced at 6 h post-ES challenge (Fig. 4B).

Since oxidative stress is the direct consequence of ES challenge in the neuronal system, we then looked at the influence of both ES and LBP pretreatment on the key oxidative stress markers, CAT and iNOS. For CAT, ES did not affect its basal expression at 2 h postchallenge but significantly inhibited this antioxidant at 6 h postchallenge, implying an increased oxidative stress status in BV-2 cells (Fig. 4C, D). This phenomenon was partly abolished by the addition of LBP, autophagic inhibitor

3-MA, or agonist rapamycin. For iNOS, a key linker of oxidative stress and inflammation, its level was significantly enhanced at both time points post-ES but ameliorated by LBP. Rapamycin further strengthened this beneficial effect of LBP (Fig. 4C, D). It should be noted that ED1 was activated by ES at 6 h postchallenge, which means an activated status of the microglia by the electric field. This was attenuated by LBP or rapamycin addition (Fig. 4C, D).

For the protein level change of key members of the autophagy pathway, such as Atg5, beclin-1, and LC3B, their level changes were consistent with the LC3B fluorescence alteration during the experiment (Figs. 3 and 4E, F). When they were inhibited by 3-MA, their levels could also be recovered by the pretreatment with LBP, indicating a potent autophagic inductive ability of this natural compound (Fig. 4E, F). Rapamycin treatment enhanced all of these markers in all groups. The changes of p62 protein expression, a substrate of the autophagic pathway, were inverted with the changes of other autophagic markers (Fig. 4E, F).

MAPK Pathway Was Involved in the
Protective Actions From LBP

The MAPK pathway is considered to be both regulator and downstream target of the autophagic pathway. To examine its involvement in ES-induced microglia damage and LBP-mediated protection of BV-2 cells, we measured the changes of MAPK pathway members ERK and p38 MAPK in each group after 2 or 6 h of ES. In the 2-h groups, both ES and LBP pretreatment did not significantly change ERK and p38 MAPK levels. However, after 6 h, the phosphorylated level of ERK was inhibited while the level of phosphorylated p38 MAPK was induced, consistent with the concept that ERK and p38 MAPK are beneficial for cell survival and damage, respectively (Fig. 5). When autophagy was inhibited by 3-MA, the phosphorylation level of ERK was inhibited at 2 h but not 6 h post-ES challenge, indicating that ERK was involved in the acute phase of ES-induced autophagic regulation (Fig. 5). This result was confirmed by the rapamycin-treated group that the basal phosphorylation of ERK was enhanced at 2 h post-ES challenge (Fig. 5A). At 6 h post-ES, both phosphorylation of ERK and p38 MAPK was enhanced by LBP or rapamycin,

FACING PAGE
Figure 4. LBP attenuates ES-induced apoptosis and oxidative stress through regulating autophagy. (A, B) Change of caspase 3/7 activity in BV-2 cell groups with ES, LBP, autophagic inhibitor 3-MA, or autophagic agonist rapamycin ($n=4$ for each group). (C) Representative Western blot pictures for the protein expression change of CAT, iNOS, and ED1 (cluster of differentiation 68; CD68) in BV-2 cell groups with ES, LBP, 3-MA, or rapamycin. Cells were collected 2 h after the ES challenge. (D) Western blot pictures of CAT, iNOS, and ED1 of cells collected 6 h after the ES challenge. (E) Western blot pictures of Atg5, p62, beclin-1, and LC3B of cells collected 2 h after the ES challenge. (F) Western blot pictures of Atg5, p62, beclin-1, and LC3B of cells collected 6 h after the ES challenge. *, **, ***Significant changes between indicated groups ($p<0.05$, $p<0.01$, $p<0.001$), respectively. ES/E, electric stimulation; L, LBP; GAPDH, glyceraldehyde 3-phosphate dehydrogenase.
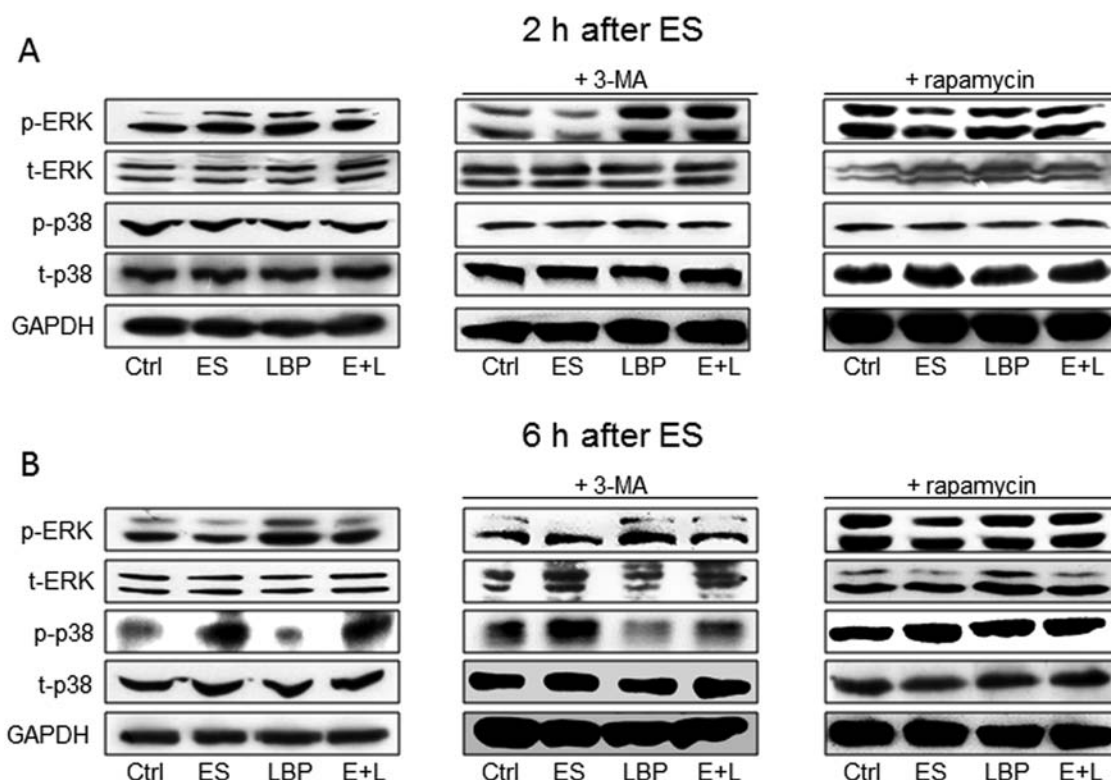
Figure 5. MAPK pathway is involved in LBP regulated autophagy after ES in BV-2 cells. (A) Representative Western blot pictures of phosphorylated ERK, total ERK, phosphorylated p38 MAPK, and total p38 MAPK in BV-2 cell groups with ES, LBP, 3-MA, or rapamycin. Cells were collected 2 h after the ES challenge. (B) Representative Western blot pictures of phosphorylated ERK, total ERK, phosphorylated p38 MAPK, and total p38 MAPK of cells collected 6 h after the ES challenge. ES/E, electric stimulation; L, LBP.

suggesting that induced autophagy could upregulate the entire MAPK pathway in the middle to late phase of ES challenge (Fig. 5B). Total levels of both ERK and p38 MAPK were not affected by ES and/or LBP in all groups. Collectively, our data showed that MAPK exerted diversified functions on ES-induced microglial injury and LBP-mediated autophagic alteration.

DISCUSSION

Visual prosthesis is one of the most exciting achievements for blindness and visual impairment therapy in the past 40 years. Although a number of successful application cases have been reported in recent years, including increased visual acuity and safety after therapy (9,10), it is still difficult to avoid possible redox and physical damage at and near the implanting sites (5). In addition, smaller electrodes often mean higher charge density, which may cause severer tissue damages. Thus, delineating the effect and mechanism for ES-induced visual injury is crucial for the further development of this technique.

Autophagy can be rapidly activated in response to stress and damage in order to maintain tissue homeostasis. Appropriate autophagic response is beneficial for the survival of cells and self-renewal of the body. However,

when it is insufficient or hyperactivated, neurodegeneration may occur due to a complicated signaling network (32). Previous studies have proven that autophagy was important for the increased survival ratio and attenuated degeneration of RGC postdamage (12,23), indicating that autophage is a double-edged sword in the neuronal system (22). In the current study, we demonstrated that in the acute response phase (2 h) after ES, cellular autophagy was elevated to initiate endogenous protective mechanisms. However, when the treatment duration was prolonged (6 h), endogenous autophagy level was inhibited due to the electric-induced damage. Those damages included inflammatory, oxidative, and apoptotic responses, as well as the activation of the MAPK pathways. These results were consistent with a very recent study indicating that graphene quantum dots (GODs) could induce inflammation, oxidative stress, and apoptosis in macrophage through regulating autophagy and p38 MAPK/nuclear factor κ-light-chain-enhancer of activated B-cells (NF-κB) pathways (17). Another study also found that autophagic responses were induced in damaged murine optic nerve, which was closely associated with the protection of RGCs. However, when Atg5 was knocked out, the survival ratio of RGCs was significantly reduced (20). Collectively, our

investigations confirmed the beneficial roles of autophagy in ES-induced microglial injury.

The protective and therapeutic effects of LBP on both neuronal system and the liver have been demonstrated by us in several kinds of diseases (8,14,27,31). Besides its potent ability in immunological regulation, LBP can also act as antioxidant and autophagic regulator. For example, in non-alcoholic fatty liver disease, consumption of LBP significantly restored the autophagic level inhibited by metabolic disorders, which was strongly related to the attenuated hepatic damages (29). In this study, in the acute phase, pretreatment with LBP further enhanced the autophagic level elevated by the electric stimulation of BV-2 cells. After 6 h of the treatment, LBP significantly restored the autophagy inhibited by the ES. Interestingly, when autophagy was inhibited or further activated by 3-MA or rapamycin, the beneficial effects of LBP on BV-2 cells were abolished or stabilized, respectively. These data confirmed the key role of autophagy in LBP-mediated BV-2 cell protections against damaging high electric field.

In conclusion, our study found that [1] high level of electric stimulation was injurious to microglia cells, which may induce inflammation, oxidative stress, and apoptosis events; and [2] treatment with LBP was able to protect microglia cells from electric stimulation-induced damages through modulating autophagy and MAPK pathways. This study may shed light on future clinical application of visual prosthesis and selection of food supplements for the therapy of blindness or other visual impairments.

REFERENCES

1. Block, M. L.; Zecca, L.; Hong, J. S. Microglia-mediated neurotoxicity: Uncovering the molecular mechanisms. Nat. Rev. Neurosci. 8:57–69; 2007.
2. Boya, P.; González-Polo, R. A.; Casares, N.; Perfettini, J. L.; Dessen, P.; Larochette, N.; Métivier, D.; Meley, D.; Souquere, S.; Yoshimori, T.; Pierron, G.; Codogno, P.; Kroemer, G. Inhibition of macroautophagy triggers apoptosis. Mol. Cell. Biol. 25:1025–1040; 2005.
3. Cavuoto, J. The Market for neurotechnology: 2012–2016. In: Cavuoto, J., ed. Neurotech Reports. San Francisco, CA: Neurotech Reports; 2011:1–345.
4. Chang, R. C.; So. K. F. Use of anti-aging herbal medicine, *Lycium barbarum*, against aging-associated diseases. What do we know so far? Cell. Mol. Neurobiol. 28:643–652; 2008.
5. Cogan, S. F. Neural stimulation and recording electrodes. Annu. Rev. Biomed. Eng. 10:275–309; 2008.
6. Du, J.; Feng, L.; Yang, F.; Lu, B. Activity- and Ca(2+)-dependent modulation of surface expression of brain-derived neurotrophic factor receptors in hippocampal neurons. J. Cell Biol. 150:1423–1434; 2000.
7. Ginet, V.; Puyal, J.; Clarke, P. G.; Truttmann, A. C. Enhancement of autophagic flux after neonatal cerebral hypoxia-ischemia and its region-specific relationship to apoptotic mechanisms. Am. J. Pathol. 175:1962–1974; 2009.
8. Ho, Y. S.; Yu, M. S.; Yik, S. Y.; So, K. F.; Yuen, W. H.; Chang, R. C. Polysaccharides from wolfberry antagonizes glutamate excitotoxicity in rat cortical neurons. Cell. Mol. Neurobiol. 29:1233–1244; 2009.
9. Humayun, M. S.; Dorn, J. D.; da Cruz, L.; Dagnelie, G.; Sahel, J. A.; Stanga, P. E.; Cideciyan, A. V.; Duncan, J. L.; Eliott, D.; Filley, E.; Ho, A. C.; Santos, A.; Safran, A. B.; Arditi, Priore, L. V. D.; Greenberg, R. J. Interim results from the international trial of second sight's visual prosthesis. Ophthalmology 119:779–788; 2010.
10. Humayun, M. S.; Weiland, J. D.; Fujii, G. Y.; Greenberg, R.; Williamson, R.; Little, J.; Mech, B.; Cimmarusti, V.; Boemel, G. V.; Dagnelie, G.; de Juan, Jr., E. Visual perception in a blind subject with a chronic microelectronic retinal prosthesis. Vis. Res. 43:2573–2581; 2003.
11. Kim, K. H.; Lee, M. S. Autophagy - A key player in cellular and body metabolism. Nat. Rev. Endocrinol. 10:322–337; 2014.
12. Knoferle, J.; Koch, J. C.; Ostendorf, T.; Michel, U.; Planchamp, V.; Vutova, P.; Tönges, L.; Stadelmann, C.; Brück, W.; Bähr, M.; Lingor, P. Mechanisms of acute axonal degeneration in the optic nerve in vivo. Proc. Natl. Acad. Sci. USA 107:6064–6069; 2010.
13. Koike, M.; Shibata, M.; Tadakoshi, M.; Gotoh, K.; Komatsu, M.; Waguri, S.; Kawahara, N.; Kuida, K.; Nagata, S.; Kominami, E.; Tanaka, K.; Uchiyama, Y. Inhibition of autophagy prevents hippocampal pyramidal neuron death after hypoxic-ischemic injury. Am. J. Pathol. 172:454–469; 2008.
14. Li, S. Y.; Yang, D.; Yeung, C. M.; Yu, W. Y.; Chang, R. C.; So, K. F.; Wong, D.; Lo, A. C. *Lycium barbarum* polysaccharides reduce neuronal damage, blood-retinal barrier disruption and oxidative stress in retinal ischemia/reperfusion injury. PLoS One 6:e16380; 2011.
15. Monk, P. N.; Shaw, P. J. ALS: Life and death in a bad neighborhood. J. Nat. Med. 12:885–887; 2006.
16. Picaud, S.; Sahel, J. A. Retinal prostheses: Clinical results and future challenges. C. R. Biol. 337:214–222; 2014.
17. Qin, Y.; Zhou, Z. W.; Pan, S. T.; He, Z. X.; Zhang, X.; Qiu, J. X.; Duan, W.; Yang, T.; Zhou, S. F. Graphene quantum dots induce apoptosis, autophagy, and inflammatory response via p38 mitogen-activated protein kinase and nuclear factor-κB mediated signaling pathways in activated THP-1 macrophages. Toxicology 327:62–76; 2015.
18. Radad, K.; Moldzio, R.; Al-Shraim, M.; Kranner, B.; Krewenka, C.; Rausch, W. D. Recent advances in autophagy-based neuroprotection. Expert Rev. Neurother. 15:195–205; 2015.
19. Rodríguez-Muela, N.; Boya, P. Axonal damage, autophage and neuronal survival. Autophagy 8:286–288; 2012.
20. Rodríguez-Muela, N.; Germain, F.; Mariño, G.; Fitze, P. S.; Boya, P. Autophagy promotes survival of retinal ganglion cells after optic nerve axotomy in mice. Cell Death Differ. 19:162–169; 2012.
21. Shepherd, R. K.; Shivdasani, M. N.; Nayagam, D. A.; Williams, C. E.; Blamey, P. J. Visual prostheses for the blind. Trends Biotechnol. 31:562–571; 2013.

22. Shintani, T.; Klionsky, D. J. Autophagy in health and disease: A double-edged sword. Science 306:990–995; 2004.

23. Sternberg, C.; Benchimol, M.; Linden, R. Caspase dependence of the death of neonatal retinal ganglion cells induced by axon damage and induction of autophagy as a survival mechanism. Braz. J. Med. Biol. Res. 43:950–956; 2010.

24. Wong, Y. T.; Dommel, N.; Preston, P. J.; Lehmann, T.; Lovell, N. H.; Suaning, G. J. Microelectronic retinal prosthesis: I. A neurostimulator for the concurrent activation of multiple electrodes. Conf. Proc. IEEE Eng. Med. Biol. Soc. 1:4647–5460; 2006.

25. World Health Organization. Global data on visual impairments. Geneva, Switzerland: World Health Organization; 2010.

26. World Health Organization. Visual impairment and blindness. Geneva, Switzerland: World Health Organization; 2012.

27. Xiao, J.; Liong, E. C.; Ching, Y. P.; Chang, R. C.; So, K. F.; Fung, M. L.; Tipoe, G. L. *Lycium barbarum* polysaccharides protect mice liver from carbon tetrachloride-induced oxidative stress and necroinflammation. J. Ethnopharmacol. 139:462–470; 2012.

28. Xiao, J.; Liong, E. C.; Huang, H.; Tse, W. O.; Lau, K. S.; Pan, J.; Nanji, A. A.; Fung, M. L.; Xing, F.; Tipoe, G. L. Cyclooxygenase-1 serves a vital hepato-protective function in chemically induced acute liver injury. Toxicol. Sci. 143:430–440; 2015.

29. Xiao, J.; Xing, F.; Huo, J.; Fung, M. L.; Liong, E. C.; Ching, Y. P.; Xu, A.; Chang, R. C.; So, K. F.; Tipoe, G. L. *Lycium barbarum* polysaccharides therapeutically improve hepatic functions in non-alcoholic steatohepatitis rats and cellular steatosis model. Sci. Rep. 4:5587; 2014.

30. Xiao, J.; Zhou, Z. C.; Chen, C.; Huo, W. L.; Yin, Z. X.; Weng, S. P.; Chan, S. M.; Yu, X. Q.; He, J. G. Tumor necrosis factor-alpha gene from mandarin fish, *Siniperca chuatsi*: Molecular cloning, cytotoxicity analysis and expression profile. Mol. Immunol. 44:3615–3622; 2007.

31. Xiao, J.; Zhu, Y.; Liu, Y.; Tipoe, G. L.; Xing, F.; So, K. F. *Lycium barbarum* polysaccharide attenuates alcoholic cellular injury through TXNIP-NLRP3 inflammasome pathway. Int. J. Biol. Macromol. 69:73–78; 2014.

32. Yang, Y.; Coleman, M.; Zhang, L.; Zheng, X.; Yue, Z. Autophagy in axonal and dendritic degeneration. Trends Neurosci. 36:418–428; 2013.

33. Yang, Z.; Klionsky, D. J. Mammalian autophagy: Core molecular machinery and signaling regulation. Curr. Opin. Cell Biol. 22:124–131; 2010.